ChemComm

Accepted Manuscript

ROYAL SOCIETY OF CHEMISTRY

rsc.li/chemcomm

View Article Online
DOI: 10.1039/C9CC02372K

Journal Name

COMMUNICATION

Preferential synthesis of ethanol from syngas via dimethyl oxalate hydrogenation over an integrated catalyst

Xin Shang, Huijiang Huang, Qiao Han, Yan Xu, Yujun Zhao,* Shengping Wang, and Xinbin Ma

Received 00th January 20xx,
Accepted 00th January 20xx

DOI: 10.1039/x0xx00000x

An integrated catalyst that contains Fe_5C_2 and CuZnO-SiO_2 with a dual-bed configuration was designed for the preferential synthesis of ethanol via dimethyl oxalate hydrogenation. The cooperation of the two catalysis components remarkably inhibited the formation of various byproducts, resulting in a significantly high ethanol yield of about 98%.

Ethanol has attracted wide attention due its important application in chemical production and potential to replace gasoline as an environmentally friendly fuel.[1] ethanol production from syngas has been proposed and considered as a promising process other than fermentation of biomass or hydration of ethylene. Direct synthesis of ethanol from syngas over Rh-based,[2] Mo-based,[3] Cu-based[4] or modified F-T synthesis catalysts[5] has made great advances in recent years. However, poor selectivity of ethanol limits its industrial application. Thus, a new ethanol synthesis route from syngas via dimethyl ether (DME) and methyl acetate (MA) is developed[6, 7]. The DME synthesized from syngas is carbonylated to MA by zeolite catalysts[8, 9] and MA is sequentially hydrogenated to ethanol by Cu-based catalysts.[10] Relatively higher yield of ethanol makes it a promising route for industrial production of ethanol from syngas.[11]

Another ethanol production process from syngas via the hydrogenation of dimethyl oxalate (DMO) has been proposed as an alternative method.[12] Cu-based catalysts have been widely investigated in the hydrogenation of DMO with a selectivity of ethylene glycol (EG) up to 95%.[13, 14] The synergy of Cu species (Cu^0 and Cu^+) for H_2 dissociation and C=O adsorption on Cu-based catalysts was reported to be responsible for the higher catalytic performance in DMO hydrogenation.[15] When the hydrogenation of DMO was performed at higher temperature and H_2/DMO, more ethanol can be formed with a selectivity of 83% by deep hydrogenation of EG on Cu-based catalyst.[16] As higher reaction temperature (~553 K) is necessary for the synthesis of ethanol from DMO hydrogenation, the formation of C3-4OH via the Guerbet reaction would be highly facilitated by the surface basic sites on the Cu-based catalysts.[17] Li's group[18] achieved a high ethanol yield of 95% by using an bifunctional catalyst (Cu nanoparticles inlaid mesoporous Al_2O_3) and 1,4-dioxane instead of methanol as the solvent. The influence of support has been also reported by the same group.[19] These works provide a meaningful instruction for developing new technology for ethanol production. Although Cu-based catalysts perform well in the conversion of DMO, how to further improve its selectivity to ethanol is still a big challenge for a process with the presence of methanol from an industrial viewpoint.[20, 21]

Recently, Liu *et al.*[22] developed a molybdenum carbide catalyst for the hydrogenation of DMO to ethanol with an ethanol yield of 70% at 473 K. They found that high activity of Mo_2C-based catalysts in C-C cleavage can lead to the decomposition of DMO and lower ethanol selectivity. In our previous work, a highly efficient iron carbide catalyst was prepared for DMO hydrogenation to ethanol with a selectivity of 90%.[23] Meanwhile, it was found that the presence of Fe_5C_2 lead to the formation of ethanol via the hydrogenation of intermediate MA instead of EG. The Fe_5C_2 catalyst exhibited a different reaction path in comparison with Cu-based catalyst (scheme 1).

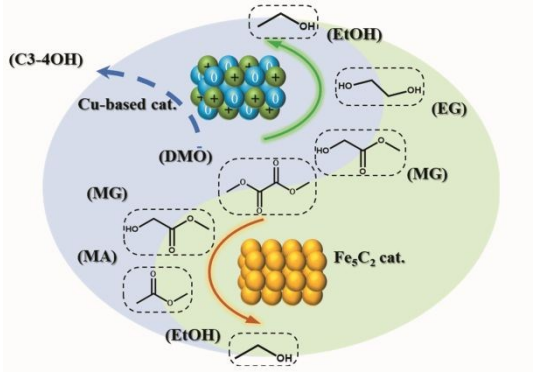

Scheme 1 The reaction pathway of hydrogenation of DMO on Fe_5C_2 and Cu-based catalyst.

[a] *Key Laboratory for Green Chemical Technology of Ministry of Education, Collaborative Innovation Center of Chemical Science and Engineering, School of Chemical Engineering and Technology, Tianjin University, Tianjin 300072, China. E-mail: yujunzhao@tju.edu.cn Address here.*

† Electronic Supplementary Information (ESI) available: Experimental details and characterization data. See DOI: 10.1039/x0xx00000x

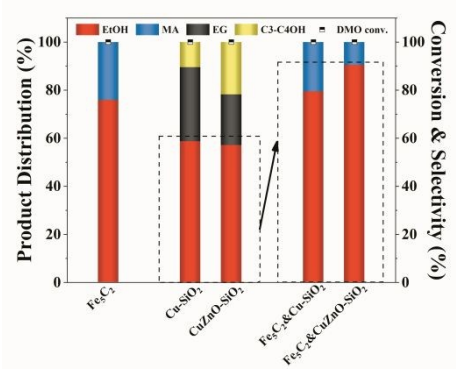

Fig. 1 Catalytic performances of various Cu-based catalysts and the combination of Fe_5C_2 and Cu-based catalysts. Reaction conditions: T=533 K, H_2/DMO=180, WLHSV=0.8 h^{-1}, P=2.5 MPa, Fe_5C_2 /Cu-based catalysts was 5/2 (mass).

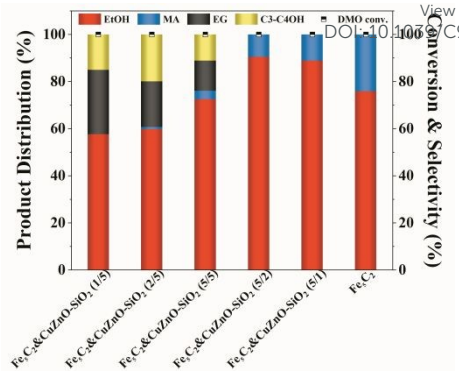

Fig. 2 Catalytic performances of the combination of Fe_5C_2 and CuZnO-SiO_2 with different mass ratios. Reaction conditions: T=533 K, H_2/DMO=180, WLHSV=0.8 h^{-1}, P=2.5 MPa.

In addition, some bifunctional catalysts or integrated systems for the conversion of C1 molecules to lower olefins[24] or liquid fuels[25] have been reported, but the concept of integrated catalysis has never been reported in selective synthesis of ethanol via DMO hydrogenation. Since Fe_5C_2 is an effective catalyst for the DMO conversion and MA is the key intermediate product in the consecutive hydrogenation system, a coupling of Fe_5C_2 and copper-based catalyst could be a rational strategy to ensure a higher ethanol selectivity in DMO hydrogenation. Herein, an integrated catalyst that contains Fe_5C_2 and CuZnO-SiO_2 with a dual-bed configuration is fabricated for the hydrogenation of DMO and a significantly high selectivity to ethanol (98%) was achieved, which is beyond all of the reported results. The effect of integration manner and the reaction paths over the integrated catalyst were also well investigated. The achievements suggest a promising prospect for its practical application.

To gain an insight into the effect of Fe_5C_2, the performance of Cu-based catalysts before and after Fe_5C_2 introduced was investigated in the hydrogenation of DMO. And the sole Fe_5C_2 was also tested in the hydrogenation for a comparison. As shown in Fig. 1, with the Cu-SiO_2 as the sole catalyst, ethanol, EG and C3-4OH were the major products. The selectivity of ethanol was very low (58.7%) and considerable amount of EG was produced due to relatively lower reaction temperature (533 K). C3-4OH (10.5%) was formed as a result of Guerbet reaction over the surface basic sites of catalyst (Fig. S3, ESI†). The selectivity of ethanol over the sole CuZnO-SiO_2 was similar as that of Cu-SiO_2, and the higher selectivity of C3-4OH (21.8%) could be ascribed to the formation of more basic sites because of the introduction of Zn (Fig. S3, ESI†). The sole Fe_5C_2 were also tested for the hydrogenation of DMO at the same conditions and the obtained ethanol selectivity was 75.9% with MA as major by-product. These results indicated that it was quite a different reaction pathway over Fe_5C_2 catalysts that the DMO was first hydrogenated to MA instead of EG on the Fe_5C_2 surface. However, it was difficult for the further hydrogenation of MA to ethanol on Fe_5C_2, so that higher selectivity to MA (24.1%) was obtained. On the other hand, when the Fe_5C_2 was introduced on the top of the Cu-based catalyst bed, the product distribution for the two Cu-based catalysts presented a significant change. The major products change to ethanol and MA in these two cases and the selectivity of ethanol was significantly improved from 40-60% to 80-90%. These results suggested a cooperation effect of the integrated catalyst, that Fe_5C_2 catalyst ensure the conversion of DMO and Cu-based catalysts prompt the further hydrogenation of intermediate MA to ethanol. The absence of methyl glycolate (MG) and EG implied that the Fe_5C_2 is enough active for the conversion of DMO and MG, preventing the formation of EG via the DMO/MG hydrogenation on Cu-based catalyst. Obviously, the formation of C3-4OH has also been efficiently inhibited on the integrated catalyst.

To further understand how the integrated catalyst performs in the hydrogenation of DMO, the mass ratio of two components (Fe_5C_2 and CuZnO-SiO_2) was tuned to investigate its effect on the catalytic performance. As shown in Fig. 2, when various mass ratios of Fe_5C_2 to CuZnO-SiO_2 were applied in the hydrogenation, the product distribution changed significantly at the same reaction conditions. When the mass ratio of Fe_5C_2 to CuZnO-SiO_2 increased from 1/5 to 5/5, the selectivity of ethanol kept increasing, accompanied by a drastic dropping of EG and C3-4OH selectivity. In this range of mass ratio, the amount of Fe_5C_2 was not yet enough to provide active sites for the conversion of DMO or MG, so unreacted DMO or MG was hydrogenated to EG on the CuZnO-SiO_2 catalyst bed, leading to the generation of C3-4OH as well on the basic sites of CuZnO-SiO_2.[17] However, as Fe_5C_2/CuZnO-SiO_2 increased further (from 5/2 to sole Fe_5C_2), there was a significant decrease of the ethanol selectivity (from 90.5% to 75.9%) accompanied by the increase of MA. In fact, the ratio of 5/2 presented better ethanol

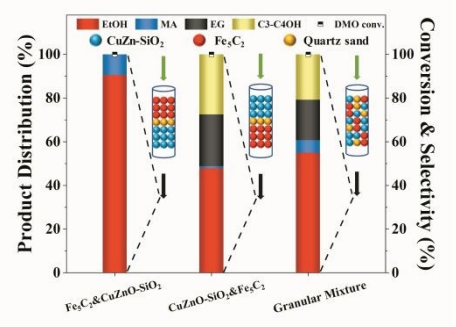

Fig. 3 Influence of the integration manner of the active components on catalytic behaviours under the same conditions. Reaction conditions: T=533 K, H_2/DMO=180, WLHSV=0.8 h^{-1}, P=2.5 MPa, Fe_5C_2/CuZnO-SiO_2 was 5/2 (mass).

View Article Online
DOI: 10.1039/C9CC02377K

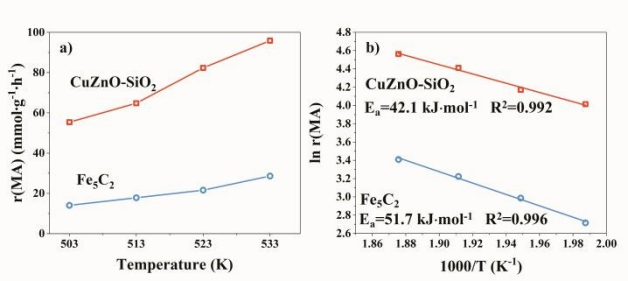

Fig. 4 The kinetic study. (a) Reaction rate for two components at various temperatures. (b) Reaction rate constant for Arrhenius plots. Reaction condition for $CuZnO\text{-}SiO_2$: H_2/MA=30, WLHSV=10 h^{-1}, P=2.5 MPa. Reaction condition for Fe_5C_2: H_2/MA=30, WLHSV=4 h^{-1}, P=2.5 MPa.

selectivity than any other ratios. Therefore, it can be concluded that Fe_5C_2 plays an important role in the total conversion of DMO and MG, due to the extremely high selectivity to MA in hydrogenation of MG (as shown in Scheme 1). But it presented relatively lower activity in hydrogenation of MA than $CuZnSiO_2$ catalyst. A cooperative effect is enhanced by an optimal ratio which ensures the complete conversion of DMO/MG into MA/ethanol on Fe_5C_2 and inhibits the formation of by-products via DMO/MG on $CuZnO\text{-}SiO_2$. Moreover, enough and efficient sites for MA conversion might request the presence of certain amount of Cu-based catalyst, otherwise, it will be hard to improve ethanol selectivity, e.g. the sole Fe_5C_2 catalyst strategy.

To further verify the effect of the integrated catalyst on ethanol selectivity and products distribution, the reaction using Fe_5C_2 and $CuZnO\text{-}SiO_2$ with different integration manners was performed the same reaction conditions. As a result, the selectivity of ethanol and the product distribution were affected markedly by the integration manner of the active components. As shown in Fig. 3, by using the dual-bed configuration with $CuZnO\text{-}SiO_2$ packed below Fe_5C_2 (Fe_5C_2&$CuZnO\text{-}SiO_2$), the selectivity to ethanol reached 90.5%. On the contrary, the dual-bed configuration with Fe_5C_2 packed below $CuZnO\text{-}SiO_2$ ($CuZnO\text{-}SiO_2$&Fe_5C_2) showed a much lower selectivity to ethanol (47.8%). The drastic drop of the ethanol selectivity should be attributed to the formation of more EG and C3-4OH. For the reaction on the $CuZnO\text{-}SiO_2$&Fe_5C_2, the conversion of DMO occurred on $CuZnO\text{-}SiO_2$ with the generation of EG and C3-4OH, which is difficult to be further converted to ethanol over Fe_5C_2 (Fig. S6, ESI†), resulting in an extremely lower ethanol selectivity. As for the reaction on granular mixture of Fe_5C_2 and $CuZnO\text{-}SiO_2$, DMO contacted with two components randomly. However, more DMO was preferentially converted into EG and C3-4OH on $CuZnO\text{-}SiO_2$ catalyst, which could be attributed to the higher adsorption ability of copper species than Fe_5C_2 site. These results suggest that a reasonable integration manner can ensure the conversion of DMO on Fe_5C_2 with high selectivity of ethanol.

As for the different products distribution obtained on various integrated catalyst, the different reaction paths on Fe_5C_2 and $CuZnO\text{-}SiO_2$ should be the main reason. The hydrogenation of DMO over Fe_5C_2 favours the formation of MA instead of EG. Unfortunately, Fe_5C_2 seems not a high active catalyst for the further hydrogenation of intermediate MA to ethanol. While, a copper-based catalyst packed following the Fe_5C_2 can effectively enhance MA hydrogenation. To get insight into the reaction mechanism, the kinetic properties (reaction rate and apparent activation energy) of the two catalyst on MA hydrogenation were examined and calculated. As shown in Fig. 4, much higher reaction rate was observed on $CuZnO\text{-}SiO_2$, whose apparent activation energy (42.1 kJ·mol^{-1}) was much lower than that of Fe_5C_2 (51.7 kJ·mol^{-1}). It indicated that $CuZnO\text{-}SiO_2$ can provide much more efficient active sites than Fe_5C_2 for MA conversion. These results offered reasonable explanations for better catalytic performance of integrated catalyst.

For the in-series packed Fe_5C_2&$CuZnO\text{-}SiO_2$ catalyst, the resident time of the reactants on various catalyst components could affect the product distribution. Therefore, Fe_5C_2&$CuZnO\text{-}SiO_2$ was tested by carrying out the reaction at varying WLHSV (weight liquid hourly space velocity). As shown in Fig. 5a, the ethanol selectivity decreases gradually as increasing the space velocity. While the selectivity of MA exhibited an increasing trend at first followed by a decrease. No any EG or C3-4OH was detected until the WLHSV was beyond 1.0 h^{-1}, when the selectivity of EG and C3-4OH showed a quick increase. These results suggested that the conversion of DMO over Fe_5C_2 was completed at WLHSV lower than 1.0 h^{-1}. In contrast, DMO cannot be fully converted over Fe_5C_2 at much higher WLHSV, since the contact time was not long enough, so that unreacted DMO or MG was hydrogenated on $CuZnO\text{-}SiO_2$ with the formation of more EG and C3-4OH. Therefore, an optimal contact time is necessary to ensure the total conversion of DMO and MG over Fe_5C_2, which is vital for obtaining higher ethanol selectivity on the integrated catalyst. In addition, the integrated catalyst was tested at varying reaction temperature from 513 K to 533 K (Inset of Fig. 5a). When the reaction was performed at lower temperature (513 K), a large amount of EG and C3-4OH were formed and no MA was found in the products. However, higher temperature benefits the conversion of DMO to MA over Fe_5C_2 catalyst, as well as the further hydrogenation of MA to ethanol on $CuZnO\text{-}SiO_2$. And, the selectivity to EG and C3-4OH was obviously inhibited as well. As a result, the higher temperature gave the higher ethanol selectivity in the temperature regime. It indicated that lower temperature could not ensure the total conversion of DMO or MG over Fe_5C_2, leading to the formation of EG and C3-4OH over $CuZnO\text{-}SiO_2$, as well as the poor ethanol selectivity. Consequently, sufficient

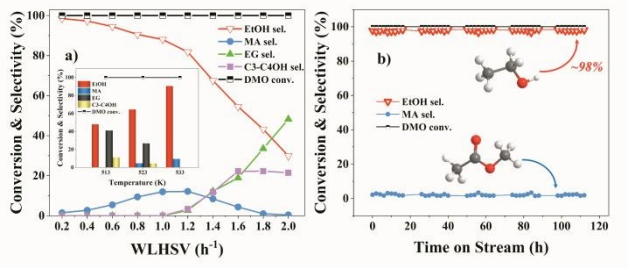

Fig. 5 Catalytic performances of the Fe_5C_2&$CuZnO\text{-}SiO_2$ integrated catalyst at (a) Varying WLHSV (T=533 K, H_2/DMO=180, P=2.5 MPa). Inset: Varying temperatures (H_2/DMO=180, P=2.5 MPa, WLHSV=0.8 h^{-1}). (b) Stability of the Fe_5C_2&$CuZnO\text{-}SiO_2$ integrated catalyst. (T=573 K, H_2/DMO=180, WLHSV=0.6 h^{-1}, P=2.5 MPa). Fe_5C_2 and $CuZnO\text{-}SiO_2$ was 5/2 (mass).

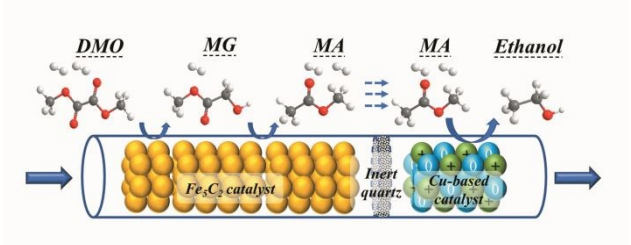

Scheme 2 The reaction mechanism of hydrogenation of DMO over integrated catalyst.

contact time and suitable reaction temperature are necessary to ensure high selectivity of ethanol. An unexpected high ethanol yield of 98% was obtained on the integrated catalyst Fe_5C_2&CuZnO-SiO_2 at 0.2 h^{-1} and 533 K. This is beyond any of reported results for the synthesis of ethanol via DMO hydrogenation. Fig. 5b exhibits an excellent stability of the integrated catalyst Fe_5C_2&CuZnO-SiO_2 in the synthesis of ethanol via DMO hydrogenation (Fig. S9, ESI†). The selectivity of ethanol kept constant with the total conversion of DMO during the lifespan test. These results suggest a promising potential for the industry application of the integrated catalyst strategy.

A possible scheme was proposed for the highly synthesis of ethanol via consecutive DMO hydrogenation reaction over Fe_5C_2&CuZnO-SiO_2 integrated catalyst (Scheme 2). The higher ability of Fe_5C_2 in activating the hydroxyl group of MG than its carbonyl group was reported in our previous work[23]. As a result, the total conversion of DMO and MG is confined on Fe_5C_2 of the integrated catalyst, and the intermediate MA is formed instead of EG. Thus, the side reactions, such as the Guerbet reaction on Cu-based catalyst, is also avoided since both DMO and EG are hardly existed. The CuZnO-SiO_2 component integrated following Fe_5C_2 presents a high activity for the hydrogenation of MA to ethanol because of its lower energy barrier for MA activation. The coupling of two reactions is achieved with unexpected high yield of ethanol by using a suitable integrated catalyst Fe_5C_2&CuZnO-SiO_2, on which the limitation of Fe_5C_2 in MA conversion, as well as the drawback of CuZnO-SiO_2 in the formation of by-products can be well overcome.

In summary, we presented a new strategy to achieve significantly high ethanol yield by applying the Fe_5C_2&CuZnO-SiO_2 integrated catalyst in the hydrogenation of DMO to ethanol. The main intermediate product was MA instead of EG due to the presence of Fe_5C_2 at top of Cu-based catalyst. Then, the CuZnO-SiO_2 help convert the generated MA into ethanol with a higher activity and selectivity because of the lower energy barriers for MA conversion. The formation of undesired products such as C3-4OH and EG was efficiently suppressed by ensuring the total conversion of DMO and MG on Fe_5C_2 catalyst bed. The practical cooperation between Fe_5C_2 and CuZnO-SiO_2 is necessary to obtain a high ethanol selectivity. At the optimized reaction conditions, the selectivity of ethanol can reach approximately 98% at DMO conversion of 100% by using the integrated catalyst. The integrated catalyst also exhibited excellent stability in the DMO hydrogenation. This feasible and efficient strategy may provide an inspiration on the rational design of industrial technology for the preferential synthesis of ethanol via DMO hydrogenation.

View Article Online
DOI: 10.1039/C9CC02372K

We are grateful to the financial support from the National Natural Science Foundation of China (21878227, U1510203).

Conflicts of interest

There are no conflicts to declare.

Notes and references

1. A. E. Farrell, R. J. Plevin, B. T. Turner, A. D. Jones, M. Hare and D. M. Kammen, *Science*, 2006, **311**, 506.
2. D. Mei, R. Rousseau, S. M. Kathmann, V.-A. Glezakou, M. H. Engelhard, W. Jiang, C. Wang, M. A. Gerber, J. F. White and D. J. Stevens, *Journal of Catalysis*, 2010, **271**, 325-342.
3. N. Wang, K. Fang, D. Jiang, D. Li and Y. Sun, *Catalysis Today*, 2010, **158**, 241-245.
4. R. Zhang, G. Wang and B. Wang, *Journal of Catalysis*, 2013, **305**, 238-255.
5. W. Wang, Y. Wang and G.-C. Wang, *PCCP*, 2018, **20**, 2492-2507.
6. W. Zhou, J. Kang, K. Cheng, S. He, J. Shi, C. Zhou, Q. Zhang, J. Chen, L. Peng, M. Chen and Y. Wang, *Angew Chem Int Ed Engl*, 2018, **57**, 12012-12016.
7. X. San, Y. Zhang, W. Shen and N. Tsubaki, *Energy & Fuels*, 2009, **23**, 2843-2844.
8. M. Boronat, C. Martínez-Sánchez, D. Law and A. Corma, *J. Am. Chem. Soc.*, 2008, **130**, 16316-16323.
9. T. He, P. Ren, X. Liu, S. Xu, X. Han and X. Bao, *Chemical Communications*, 2015, **51**, 16868-16870.
10. Y. Zhao, B. Shan, Y. Wang, J. Zhou, S. Wang and X. Ma, *Industrial & Engineering Chemistry Research*, 2018, **57**, 4526-4534.
11. X. Li, X. San, Y. Zhang, T. Ichii, M. Meng, Y. Tan and N. Tsubaki, *ChemSusChem*, 2010, **3**, 1192-1199.
12. H. Yue, X. Ma and J. Gong, *Acc. Chem. Res.*, 2014, **47**, 1483-1492.
13. X. Zheng, H. Lin, J. Zheng, X. Duan and Y. Yuan, *ACS Catalysis*, 2013, **3**, 2738-2749.
14. J. Lin, X. Zhao, Y. Cui, H. Zhang and D. Liao, *Chemical Communications*, 2012, **48**, 1177-1179.
15. A. Yin, X. Guo, W.-L. Dai and K. Fan, *The Journal of Physical Chemistry C*, 2009, **113**, 11003-11013.
16. J. Gong, H. Yue, Y. Zhao, S. Zhao, L. Zhao, J. Lv, S. Wang and X. Ma, *J Am Chem Soc*, 2012, **134**, 13922-13925.
17. Y. Song, J. Zhang, J. Lv, Y. Zhao and X. Ma, *Industrial & Engineering Chemistry Research*, 2015, **54**, 9699-9707.
18. Y. Zhu, X. Kong, X. Li, G. Ding, Y. Zhu and Y.-W. Li, *ACS Catalysis*, 2014, **4**, 3612-3620.
19. Y. Zhu, Y. Zhu, G. Ding, S. Zhu, H. Zheng and Y. Li, *Applied Catalysis A: General*, 2013, **468**, 296-304.
20. S. Zhao, H. Yue, Y. Zhao, B. Wang, Y. Geng, J. Lv, S. Wang, J. Gong and X. Ma, *Journal of Catalysis*, 2013, **297**, 142-150.
21. J. Zheng, J. Zhou, H. Lin, X. Duan, C. T. Williams and Y. Yuan, *The Journal of Physical Chemistry C*, 2015, **119**, 13758-13766.
22. Y. Liu, J. Ding, J. Sun, J. Zhang, J. Bi, K. Liu, F. Kong, H. Xiao, Y. Sun and J. Chen, *Chemical Communications*, 2016, **52**, 5030-5032.
23. J. He, Y. Zhao, Y. Wang, J. Wang, J. Zheng, H. Zhang, G. Zhou, C. Wang, S. Wang and X. Ma, *Chemical Communications* , 2017, **53**, 5376-5379.
24. F. Jiao, J. Li, X. Pan, J. Xiao, H. Li, H. Ma, M. Wei, Y. Pan, Z. Zhou, M. Li, S. Miao, J. Li, Y. Zhu, D. Xiao, T. He, J. Yang, F. Qi, Q. Fu and X. Bao, *Science*, 2016, **351**, 1065-1068.
25. P. Gao, S. Li, X. Bu, S. Dang, Z. Liu, H. Wang, L. Zhong, M. Qiu, C. Yang, J. Cai, W. Wei and Y. Sun, *Nature Chemistry*, 2017, **9**, 1019.